A Macroscopic Relationship for Preferential Flow in the Vadose Zone: Theory and Validation

Liu, Hui-Hai[1] and Zhang, Renduo[2]

[1]Earth Science Division, Lawrence Berkeley National Laboratory, Berkeley, California, USA;
[2]School of Environmental Science and Engineering, Sun Yat-Sen (Zhongshan) University, Guangzhou, P.R. China

Preferential flow commonly observed in unsaturated soils allows rapid movement of solute from the ground surface or vadose zone to the groundwater, bypassing a significant volume of unsaturated soil and increasing the risk of groundwater contamination. A variety of evidence indicates that complex preferential flow patterns observed from fields are fractals. This paper discusses a macroscopic relationship for modeling preferential flow in the vadose zone. Conceptually, the flow domain can be divided into active and inactive regions. Flow occurs preferentially in the active region (characterized by fractals), and inactive region is simply bypassed. The portion of the active region was found to be a power function of saturation. The validity of this macroscopic relationship is demonstrated by its consistency with field observations and the related numerical experiments.

preferential flow, constitutive relations, vadose zone hydrology

1 Introduction

It has been recognized that preferential flow is common for natural unsaturated soils. Preferential flow results in that liquid water propagates quickly to significant depths while bypassing large portions of the vadose zone, and solute travel times from the contamination source (located in soil surface or vadose zone) to groundwater are shorter than a prior expected[6]. Because of the important effects of this flow process on groundwater contamination (a important issue for water resources management), preferential flow has been a major research area in the vadose zone hydrology community for many years[30].

Field-scale preferential flow is caused by a number of well-known mechanisms. First, under flooding and/or high-infiltration-rate conditions, water can flow very quickly along macropores (such as cracks and fissures) in structured soils[2,3,6,7,21]. Second, because of the high nonlinearity of the unsaturated flow process, an infiltrating water front can become unstable and split into "fingers" even for relatively homogeneous, structureless soils[4,8,11,34]. Third, the spatial variability of soil properties also causes highly non-uniform flow patterns corresponding to preferential flow paths[33]. At the field scale, a combination of these three mechanisms likely contributes to the observed preferential flow processes, although one or two of them may be dominant mechanisms for a given testing site.

Because of its complexity, preferential flow and the associated solute transport are probably the most frustrating processes in terms of hampering accurate predictions of contaminant transport in the vadose zone[30]. We believe that the major limitation of the commonly used modeling approaches is their incapability to parameterize the preferential flow process in an accurate, yet practical manner. To resolve this issue, we have developed a macroscopic relationship describing preferential flow pattern and other related parameters that allows for successfully modeling large-scale unsaturated flow processes in vadose zone[13-15]. This paper discusses the derivation for the relationship and its validation.

Received April 5, 2008; accepted September 4, 2008
doi:
†Corresponding author (email: hhliu@lbl.gov)

2 Fractal flow patterns and preferential flow process

Fractals have been shown to provide a common language for describing many different natural and social phenomena[16]. While a vast literature exists on the validity of the fractal concept for a great number of fields, fractals have been found to be useful for representing many spatial distributions in subsurface hydrology, including soil particle size distribution, roughness of fracture surface, distribution of permeability in heterogeneous formations, and large-scale solute dispersion processes[18,19,20,24,26,27,32].

Recent studies have also suggested that complex preferential flow patterns in unsaturated systems can be characterized by fractals. Ref. [10] may be the first authors to report in the vadose zone hydrology community that the geometry of dyed flow patterns in two-dimensional images of soil profiles could be characterized by fractals. Refs. [7,25] indicated that solute leaching patterns, observed from field plots, could be well represented by a diffusion-limited aggregation (DLA) model[35]. It has been documented that DLA generates fractal patterns[5,7,17]. Refs. [21,22] also noticed that the dye penetrations for two test sites (corresponding to a clayey and a sandy soil) are characterized by power-law mean power spectrum, a signature of fractal pattern. Ref. [23] reported that a field observation of dyed flow pattern in an unsaturated test site is characterized by multi-fractals. This finding is consistent with that in many cases spatial distributions of hydraulic conductivity are multi-fractals[12].

Related to preferential flow in unsaturated soils, fractal flow patterns have often been observed in other unsaturated and multi-phase flow systems. Ref. [9] first showed that unsaturated flow in a single vertical fracture is characterized by gravity-driven fingers, and the resulting flow patterns could be modeled by an invasion-percolation approach[36]. Again, percolation-based models generate fractal clustering patterns[31]. Viscous fingering in porous media has been experimentally shown to be fractal[5]. Ref. [29] reported that DNAPL fingering in water saturated porous media, observed from sandbox experiments, is fractal. Ref. [14] demonstrated that a spatial distribution of fractures with mineral coatings is also fractal, while fracture coating is roughly a signature of water flow paths.

3 A macroscopic relationship

As discussed in Section 2, highly non-uniform (preferential) flow patterns in unsaturated soil (and other unsaturated and multi-phase flow systems) are fractal. Therefore, it is critical to incorporate fractal flow patterns for modeling preferential flow behavior. To do so, we have developed a macroscopic relationship. The main idea is that flow domain can be divided into active and inactive regions. Flow occurs preferentially in the active region (characterized by fractals) and inactive (immobile) region is simply bypassed. The macroscopic relationship links the active region with related large-scale flow parameters. This section presents the derivation of the relationship based on the fractal flow patterns.

The key parameter for a fractal pattern is fractal dimension. Fractal dimension, d_f, is generally a noninteger and less than the corresponding Euclidean (topological) dimension of a space, D. Different kinds of definitions for fractal dimension exist (e.g., similarity dimension, Hausdorff dimension, and box dimension), although they provide very close fractal dimension values for practical applications[5]. The most straightforward definition is the so-called box dimension, based on a simple "box-counting" procedure. This dimension is determined from Equation (1) (below) by counting the number (N) of "boxes" (e.g., line segments, squares and cubes for one-, two-, and three-dimensional problems, respectively) needed to cover a spatial pattern, as a function of box size (l)[5]:

$$N(l) = \left(\frac{L}{l}\right)^{d_f} \tag{1}$$

where L refers to the size of the entire spatial domain under consideration. Figure 1 shows a box-counting procedure for a spatial pattern with d_f = 1.6, in a two-dimensional domain with size L[37].

Obviously, if a spatial pattern is uniformly distributed in space, the fractal dimension will be identical to the corresponding Euclidean dimension. In this case, the number of boxes that cover the pattern, N^*, and the box size l have the following relation

$$N^*(l) = \left(\frac{L}{l}\right)^{D} \tag{2}$$

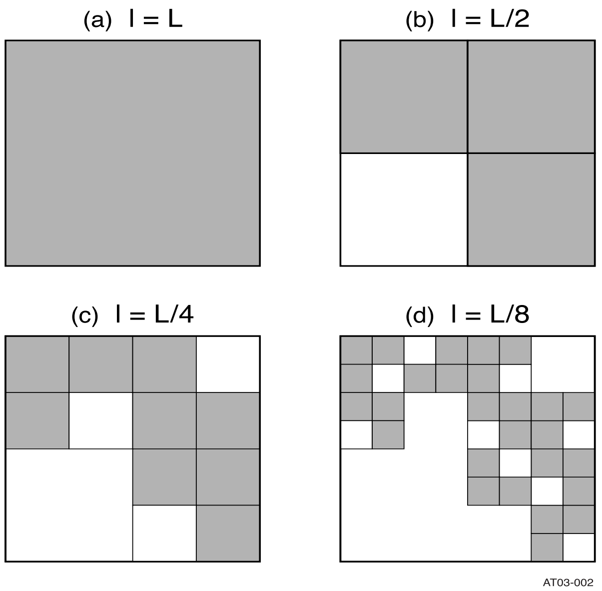

Figure 1 Demonstration of the "box" counting procedure for several box sizes.

A fractal pattern exhibits similarity at different scales. When $d_f < D$, the corresponding pattern does not fill the whole space, but only part of it (Figure 1).

To incorporate the effects of fractal flow patterns, we need to develop a simple scheme to characterize these patterns in terms of parameters relevant to water flow processes. Consider Figure 1(a) to be a gridblock containing an active flow region and the corresponding flow pattern to be fractal. In this case, only a portion of the medium within a gridblock contributes to water flow (Figure 1). This is conceptually consistent with the preferential flow process. Note that in Figure 1, a box is shadowed if it covers the active flow region.

Combining Equations (1) and (2) yields

$$[N(l)]^{1/d_f} = [N^*(l)]^{1/D} \tag{3}$$

The average active water saturation (S_e*) for the whole gridblock (Figure 1a) is determined to be

$$S_e^* = \frac{V}{l^D \phi N^*(l)} \tag{4}$$

where V is the total water volume (excluding residual water) in the active region for the gridblock (Figure 1a), and ϕ is the effective porosity (corresponding to saturated water content excluding residual water content). Similarly, the average active water saturation (S_b*) for shadowed boxes with size of l is

$$S_b^* = \frac{V}{l^D \phi N(l)} \tag{5}$$

From Figure 1, it is obvious that there exists a box size $l_1 < L$ satisfying:

$$\frac{V}{l_1^D \phi} = 1 \tag{6}$$

Based on Equations (3)–(6), the average saturation for shadowed boxes with size l_1, S_{b1}*, can be expressed by

$$S_{b1}^* = (S_e^*)^{\frac{d_f}{D}} \tag{7}$$

Because a fractal is similar at different scales, the procedure to derive Equation (7) from a gridblock with size L can be applied to shadowed boxes with the smaller size of l_1. In this case, for a given box size smaller than l_1, the number of shadowed boxes will be counted as an average number for those within the (previously shadowed) boxes with a size of l_1. Again, we can find a box size $l_2 < l_1$ to obtain a saturation relation:

$$S_{b2}^* = (S_{b1}^*)^{\frac{d_f}{D}} = (S_e^*)^{\left(\frac{d_f}{D}\right)^2} \tag{8}$$

The procedure to obtain Equation (8) can be continued until it reaches an iteration level, n^*, at which all the shadowed boxes with a size of l_n cover the active region only. The resultant average saturation for these shadowed boxes is

$$S_{bn}^* = (S_e^*)^{\left(\frac{d_f}{D}\right)^{n^*}} \tag{9}$$

By definition, S_{bn} should be equivalent to the effective water saturation (S_a) within the active region. Using f to denote the fraction of the active region within the gridblock and based on Equation (9), we have

$$f = \frac{S_e^*}{S_a} = (S_e^*)^{\gamma} \tag{10}$$

with

$$\gamma = 1 - \left(\frac{d_f}{D}\right)^{n^*} \tag{11}$$

Parameter γ is defined between zero and one. If flow pattern is uniform and does not contain preferential flow, γ will be equal to zero (corresponding to $d_f = D$ or $f = 1$). Otherwise, γ will be larger than zero and result in an f value less than one. In this case, only a portion of the flow domain corresponding to preferential flow paths actually conducts liquid water. The γ may be a complex function of soil properties, flow conditions, and scale. In this study, we assume it to be a constant for a given test site. This approximation seems to suffice for practical applications. Ref. [14] also demonstrated that this approximation is valid for fingering flow in homogeneous porous media.

Equation (10) comprises our macroscopic relationship that links the portion (f) of the region where water flow actively occurs to a macroscopic parameter, the effective water saturation S_e*. When incorporated into a continuum approach, this macroscopic relationship provides a powerful tool for describing preferential flow processes in the vadose zone[14,15].

4 Evaluation of the macroscopic relationship

The macroscopic relationship described in Section 3 has been evaluated in direct and indirect manners. The former refers to direct comparisons between Equation (10) and field observations of portion of the active region as a function of the effective saturation. The latter corresponds to comparisons between simulated (based on the relationship) and observed flow and transport results. This paper focuses on the direct evaluation that is considered to be more convincing.

To evaluate the relationship[28], field experiments were conducted at two different field sites from June of 2006 to Oct. of 2007 in Wuhan, China. Before the experiment, Site I was used for vegetation production. The soil texture was loam with visually uniform profiles. At Site II, the top 40 cm layer was loose soil, which was removed before the experiments, and the experiment soil consisted of clay. A number of infiltration tests were carried out at each site with dyed water. The sizes of infiltration plots are on the order of 100 cm x 100cm. Right after the infiltration tests were terminated, vertical soil profiles were excavated across the corresponding plot at a horizontal interval of 5 cm. The dyed soil water flow patterns were recorded and soil water saturation distributions were measured. Figure 2 shows an observed dyed water flow pattern.

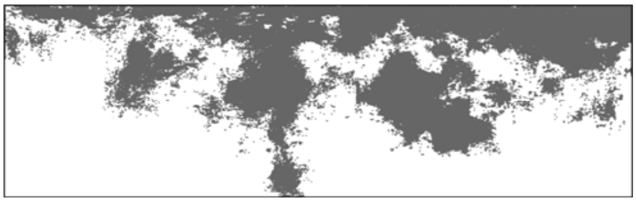

Figure 2 An observed soil-water flow pattern in a vertical cross section[28]

For a given experiment, the dyed region in a soil profile is considered the active region. At a given depth, parameter f in Equation (10) was estimated as the ratio of the length of dyed portion to the total horizontal length of the soil profile. The effective soil water saturation S_e* was estimated from measured soil-water saturation distributions (Equation [4]). In the active region, all the water, excluding the residual water content, is assumed to be mobile. Therefore, ideally experiments should be carried out under dry soil conditions (with the initial soil water saturation near the residual value). However, under field conditions, it is virtually impossible to conduct experiments under such conditions. To analyze our experimental data, it was assumed that before experiments, all water in the soil was immobile although the water content was higher than the residual water content. This assumption can be partially justified, considering that water flows much more quickly in the active (stained) region for the given test conditions. The focus of the evaluation is on whether Equation (10) is consistent with observed relations between f and S_e*. As an example, Figure 3 shows comparison results for tests conducted at Site II. Similar results were also obtained for tests conducted at Site I[28] and from other test sites[15]. Given the complexity of the flow pattern and soil-water saturation distributions (Figure 2), the matches of Equation (10) with experimental data are remarkable. The fitted values for parameter γ (Equation [10]) range from 0.66 to 0.76, which is not considered a significantly large range for a given soil type.

Our macroscopic relationship is applicable to unsaturated water flow in both natural soils and fracture networks[13,14]. As a matter of fact, the relationship was initially developed for modeling large-scale water flow in the unsaturated zone of Yucca Mountain, Nevada, USA[13,14]. Although the focus of this paper is on the water flow in soils, it may be of interest to show a recent evaluation of our relationship for a fracture network.

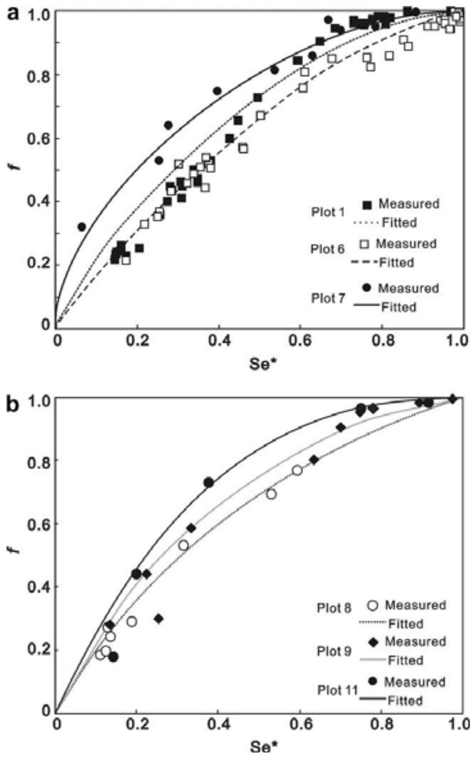

Figure 3 Matches of Equation (10) with experimental data collected from different infiltration plots at Site I[28].

Recently, Ref. [1] developed a two-dimensional multiphase lattice-Boltzmann model for analyzing flow patterns in unsaturated fracture networks with relatively simple geometries consisting of horizontal and vertical fractures (when tilt angle equals zero). The numerical experiments were conducted for different injection rates and fracture orientations. Liquid water was injected from a single point at the top of fracture networks. The details regarding modeling methodologies can be found in ref. [1]. The unique aspect of their study is that detailed flow patterns (such as film flow and effects of capillary barriers) can be simulated. Similar flow patterns and the associated water saturation distributions would be very difficult, if not impossible, to obtain for fractured rock under field conditions. To evaluate our macroscopic relationship, the value for parameter f is determined as the ratio of length of fractures that contain water to the total fracture length for a given simulation scenario. Consequently, a number of data points of parameter f as a function of effective saturation are obtained for a fracture network with a fixed title angle. Again, these data points are consistent with our macroscopic relationship. As an example, Figure 5 shows a comparison between the data points and the theoretical results (Equation [10]) for a fracture-network tilt angle of 25^0. Similar matches were found for all other tilt angles. At least for the range of numerical experiment conditions considered in ref. [1], our relationship represents data points very well.

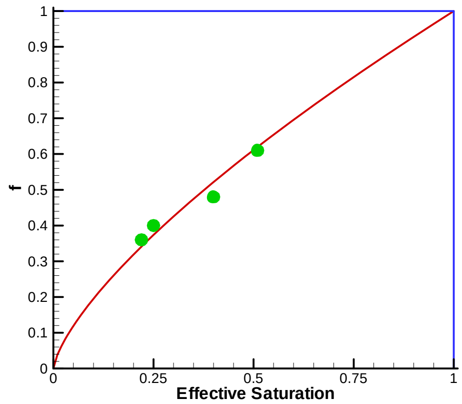

Figure 4 A comparison between simulated data points and results calculated from Equation (10) with γ =0.71.

5 Conclusion

Preferential flow and transport are common processes in unsaturated soils. Development of theoretically rigorous and practically useful approaches is a current challenge. Existing field evidence indicates that complex preferential flow patterns are fractals. This study presents our recent development of a macroscopic relationship for modeling preferential flow in the vadose zone. Conceptually, the flow domain is divided into active and inactive regions. Flow occurs preferentially in the active region and inactive region is simply bypassed. The portion of the active region was found to be a power function of saturation. The validity of this relationship is demonstrated by its consistency with field observations and the related numerical experiments. Very promising model prediction results for field-scale unsaturated flow has been obtained by incorporating the relationship into the continuum approach[14]. Further studies are needed for developing relations between the γ parameter (defined in Equation (10)) and the other soil hydraulic parameters and for relaxing the water-immobility assumption for the inactive region in models based on the developed macroscopic relationship.

Acknowledgment: This work was partially supported by the U.S. Department of Energy and LBNL under Contract No. DE-AC02-05CH11231.

1 Basağaoğlu H, Succi S, Manepally C, Fedeors R, Wyrick D Y. Sensitivity of the active fracture model parameter to fracture network orientation and injection scenarios. Hydrogeology Journal, 2009 (in Press).
2 Beven K, Germann P. Macropores and water flow in soils. Water Resources Research, 1982, 18: 1311-1325.
3 Bouma J, Dekker L W. A case study on infiltration into dry clay soil, I. Morphological observations. Geoderma, 1978, 20: 27-40.
4 de Rooij G H. Modeling fingered flow of water in soils owing to wetting front instability: a review. J. Hydrol., 2000, 231-232: 277-294.
5 Feder J. Fractals. Plenum Press, New York, 1988.
6 Flury M, Fluhler H, Jury W A, Leuenberger J. Susceptibility of soils to preferential flow of water: A field study. Water Resources Research, 1994, 30(7): 1945-1954.
7 Flury M, Flühler H. Modeling solute leaching in soils by diffusion-limited aggregation: Basic concepts and applications to conservative solutes. Water Resources Research, 1995, 31: 2443-2452.
8 Glass R J, Steenhuis T S, Parlarge J Y. Wetting front instability as a rapid and far-reaching hydrologic process in the vadose zone. J. Contam. Hydrol., 1988, 3: 207-226.
9 Glass R .J. Modeling Gravity-Driven fingering using modified percolation theory. In Proceedings of the fourth annual international conference on high level radioactive waste conference, Las Vegas, Nevada, 1993.
10 Hatano R, Booltink H W G. Using fractal dimensions of stained flow patterns in a clay soil to predict bypass flow. J. Hydrol, 1992, 135: 121-131.
11 Hillel D. Unstable flow in layered soils: A review. Hydrol. Processes, 1987, 1: 143-147.
12 Liu H H, Molz F J. Multifractal analyses of hydraulic conductivity distribution. Water Resources Research, 1997, 33: 2483-2488.
13 Liu H H, Doughty C, Bodvarsson G S. An active fracture model for unsaturated flow and transport in fractured rocks. Water Resources Research, 1998, 34: 2633–2646.
14 Liu H H, Zhang G, Bodvarsson G S. The active fracture model: Its relation to fractal flow behavior and a further evaluation using field observations. Vadose Zone Journal, 2003, 2: 259-269.
15 Liu H H, Zhang R D, Bodvarsson G S. An active region model for capturing fractal flow patterns in unsaturated soils: Model development. J Contam Hydrol, 2005, 80(1-2): 18-30.
16 Mandelbrot B B. The fractal geometry of nature. New York: W.H. Freeman, 1982.
17 Meakin P, Tolman S. Diffusion-limited aggregation. In Fractals in the natural sciences. Princeton: Princeton Univ. Press, N.J., 1989.
18 Molz F J, Boman G .K. A stochastic interpolation scheme in subsurface hydrology. Water Resources Research, 1993, 29: 3769-3774.
19 Neuman, S P. Uinversal scaling of hydraulic conductivities and dispersivities in geologic media. Water Resources Research, 1990, 26: 1749-1758.
20 Neuman S P. Generalized scaling of permeabilities: Validation and effect of support scale. Geophys. Res. Lett., 1994, 21:349-352.
21 Öhrström P, Persson M, Albergel J, Zante P, Nasri S, Berndtsson R, Olsson J. Field-scale variation of preferential flow as indicated from dye coverage. J. Hydrol., 2002, 257: 164-173.
22 Öhrström P, Hamed Y, Persson M, Berndtsson R. Characterizing unsaturated solute transport by simultaneous use of dye and bromide. J. Hydrol., 2004, 289:23-35.
23 Olsson J, Persson M, Albergel J, Berndtsson R, Zante P, Ohrstrom P, Nasri S. Multiscaling analysis and random cascade modeling of dye infiltration. Water Resources Research, 2002, 38(11): 1263. Doi:10.1029/2001WR00080.
24 Perfect E, McLaughlin N B, Kay B D, Topp G. C. An improved fractal equation for the soil water retention curve. Water Resources Research, 1996, 32:281-287.
25 Persson M, Yasuda H, Albergel H, Berndtsson R, Zante P, Nasri S, Ohrstrom P. Modeling plot scale dye penetration by a diffusion limited aggregation (DLA) model. J. Hydrol., 2001, 250:98-105.
26 Rieu M, Sposito G., 1991a. Fractal fragmentation, soil porosity, and soil water properties, 1. Theory. Soil Sci. Soc. Am. J., 1991a, 55: 1231-1238.
27 Rieu M, Sposito. Fractal fragmentation, soil porosity, and soil water properties, 2. Applications. Soil Sci. Soc. Am. J., 1991b, 55:1231-1238.
28 Sheng F, Wang K, Zhang R D, Liu H H. Characterizing soil preferential flow using iodine–starch staining experiments and the active region model. J Hydrol., 2009, 367(1-2):115-124.
29 Smith J E, Zhang Z F. Determining effective interfacial tension and predicting finger spacing for DNAPL penetration into water-saturated porous media. J. Contam. Hydrol., 2001, 48: 167-183.
30 Simunek J, Jarvis N J, van Genuchten M Th, Gardenas A. Review and comparison of models for describing non-equilibrium and preferential flow and transport in the vadose zone. J. Contam. Hydrol., 2003, 272:14-35.
31 Stauffer D, Aharony A. Introduction to Percolation Theory. Tayler & Francis, 1991.
32 Tyler S W, Wheatcraft S W. Fractal processes in soil water retention. Water Resources Research, 1990, 26:1047-1054.
33 Vogel T, Gerke H H, Zhang R, van Genuchten M Th. Modeling flow and transport in a two-dimensional dual-permeability system with spatially variable hydraulic properties. J. Hydrol., 2000, 238: 78-89.
34 Wang Z, Wu L, Harter T, Lu J, Jury W A. A field study of unsatuable preferential flow during soil water redistribution. Water Resources Research, 2003, 39(4):1075, doi:10.1029/2001WR000903.
35 Witten T A, Sander L M. Diffusion-limited aggregation: A kinetic critical phenomenon. Phys. Rev. Lett., 1981, 47:1400-1403.
36 Wilkinson D, Willewsen J F. Invasion percolation: A new form of percolation theory. J. Phys. A., 1983, 16: 3365-3376.
37 Yamamoto H, Kojima K, Tosaka H. Fractal clustering of rock fractures and its modeling using cascade process. In Scale Effects in Rock Masses 93, Pinto da Cunha (ed.). Balkema, Rotterdam, 1993.

DISCLAIMER